Silicon (2022) 14:6447–6455
https://doi.org/10.1007/s12633-021-01440-6

ORIGINAL PAPER

A Study of Thermal, and Optical Properties of $22SiO_2$- $23Bi_2O_3$-$37B_2O3$-$13TiO_2$-(5-x) LiF- x BaO Glasses

Atif Mossad Ali[1,2] · Z. A. Alrowaili[3] · Ateyyah M. Al-Baradi[4] · M. S. Al-Buriahi[5] · E. A. Abdel Wahab[6] · Kh. S. Shaaban[7]

Received: 21 August 2021 / Accepted: 24 September 2021 / Published online: 7 October 2021

Abstract
Using melt-quenching techniques, the glass system $22SiO_2$- $23Bi_2O_3$-$37B_2O_3$-$13TiO_2 - (5 - x)$ LiF- x BaO was prepared. The amorphous status of fabricated samples were established using X-ray diffraction patterns. Differential thermal analysis (glass transition temperature, crystallization temperature, and thermal stability) as well as optical properties (molar refractivity, bandgap, molar polarizability, reflection loss, metallization, electronegativity, and electron polarizability) of these glasses have been investigated. These structural changes influence the thermal properties, as we discovered. Indeed, as BaO levels rise, all the thermal parameters rise as well. With increasing BaO content, density, and refractive index rise. Bandgap energies for direct and indirect transitions reduced as the BaO content increased while Urbach energy increases. This interpretation attributable to the increment in the bond length of Ba-O. This study suggests that the fabricated glasses' optical and thermal characteristics have improved, making them suitable for a variety of applications.

Keywords Titania · Glasses · DTA · UV spectroscopy · Polarizability · Basicity

1 Introduction

Due to their unique physical, mechanical, and chemical characteristics, borosilicate glasses are one of the most examined glasses. These glasses are dopant with a wide range of modifying oxides, like transition metal oxides (TMO), and form strong glass networks. Condensed matter physics, glass science, and materials chemistry are all interested in the characteristics of these glasses. Many physicists and chemists investigated these glasses using theoretical and experimental methods. By taking the different valence states of bismuth ions, bismuth borosilicate network structures have been improved. Therefore, these glasses are appropriate for electro-optic, protection, and electronic applications [1–5].

Glass with (TMO) has been used in a wide range of applications in recent years due to its unique optoelectronic characteristics [6–9]. TiO_2 is a common glass ingredient used to improve the optics and thermal features of the glass. Small amounts of TiO_2 can have a big impact on mechanical, optical, and shielding properties, which is why glass scientists are interested in it [10–17]. Due to its different coordination states Ti^{+4}, Ti^{+5}, and Ti^{+6}, TiO_2 plays a significant role in glass systems. TiO_2 can have a completely different impact on the characteristics because of the change in coordination [10–17].

Fluoro-alkali-TiO_2-SiO_2-B_2O_3 glasses present an attractive structure for observing changes in glass behavior. Infrared spectroscopy, shielding, mechanical, and UV-spectroscopy techniques have been used to investigate the structure of these glasses [18–20]. Alkaline-TiO_2-SiO_2- B_2O_3 glasses present an attractive structure for observing changes in glass behavior. TeO_2-$LiNbO_3$-BaO-BaF2-La_2O_3 glass system is examined by Rammah et al. for its structural, optical, and shielding

✉ Kh. S. Shaaban
khamies1078@yahoo.com

[1] Physics Department, Faculty of Science, King Khalid University, Abha 61413, Saudi Arabia

[2] Department of Physics, Faculty of Science, Assiut University, 71516 Assiut, Egypt

[3] Physics Department, College of Science, Jouf University, P.O. Box: 2014, Sakaka, Saudi Arabia

[4] Department of Physics, College of Science, Taif University, P.O. Box 11099, 21944 Taif, Saudi Arabia

[5] Department of Physics, Sakarya University, Sakarya, Turkey

[6] Physics Department, Faculty of Science, Al Azhar University, P.O. Box 71524, Assiut, Egypt

[7] Chemistry Department, Faculty of Science, Al-Azhar University, P.O. Box 71524, Assiut, Egypt

properties [21]. The structural, optics, and influence of gamma irradiation of the $NaF-CaF_2-B_2O_3$ glass system are investigated by El Batal et al. [22]. Abd El-Rehim [23] and Shaaban et al. [24] examined the effects of La_2O_3 on the optical, thermal, and radiation characteristics of NaF - BaO - PbO - B_2O_3 glasses.

Using melt-quenching techniques, the glass system $22SiO_2$- $23Bi_2O_3$-$37B_2O_3$-$13TiO_2$-$(5-x)$ LiF- x BaO was prepared. The effects of increasing BaO content on optical characteristics have been evaluated. *Eopt* has been obtained in both linear and non-linear. BaO has increased at the expense of LiF, the extent of thermal in these samples has been investigated.

2 Materials and Methods

The high temperature melting method was used to create the glasses. With mol%, the glasses have the following chemical composition:

$22SiO_2$- $23Bi_2O_3$-$37B_2O_3$-$13TiO_2$-5LiF
$22SiO_2$- $23Bi_2O_3$-$37B_2O_3$-$13TiO_2$-4LiF- 1BaO
$22SiO_2$- $23Bi_2O_3$-$37B_2O_3$-$13TiO_2$-3LiF- 2BaO
$22SiO_2$- $23Bi_2O_3$-$37B_2O_3$-$13TiO_2$-2LiF- 3BaO
$22SiO_2$- $23Bi_2O_3$-$37B_2O_3$-$13TiO_2$-5BaO

For glass preparation, starting materials with purity (99.99 %) were used. Aldrich provides all raw materials used in the production of glasses. H_3BO_3 is converted to B_2O_3 after H_2O evaporation. The reagents were mixed in an electric furnace and then melted for 2 h at 1200 °C in ceramic crucibles. The homogeneous melts were then cast into a graphite mould that had been preheated. At 450 °C, the synthetic samples were annealed.

The structure of the samples was analysed using a Philips X-ray diffractometer (model PW/1710). Using CCl_4 as the buoyant medium, the glass density was determined using the Archimedes principle. A spectrophotometer (JASCO V-670 - Japan) was used to measure the UV transmittance (T) and absorbance (A) spectra of highly polished glasses from 2700 to 200 nm. The molar refractivity R_m is expressed asbandgap $E_{opt.}$, molar polarizability ($\propto_m$), and Reflection loss R_L, expressed as: $R_m = Vm\left(1-\sqrt{Eopt./20}\right), \propto_m = \left(\frac{3}{4\pi N}\right)R_m$, $R_L = \left(\frac{R_m}{Vm}\right)$. Metallization M, electronegativity (χ), electron polarizability $\propto°$, and optical basicity $\wedge$ expressed as:
$M = 1-\frac{R_m}{Vm}, \quad \chi = 0.2688E_{opt.}, \quad \propto° = -0.9\chi+3.5, and$ $\wedge = -0.5\chi+1.7$.

The DTA investigation was conducted using a micro-DTA apparatus (Shimadzu, TA-50, Japan). The measurements are accurate to within 5 °C [25].

3 Results and Discussions

3.1 Physical Investigation

The crystalline, amorphous, and mixed existence of the samples was determined using XRD. XRD of synthesized glasses in the (10–100) 2θ range is displayed in Fig. 1. Because the XRD of all synthesized glasses was similar, only the XRD for $22SiO_2$- $23Bi_2O_3$-$37B_2O_3$-$13TiO_2$-3LiF-2BaO is shown here. Because of the presence of short-range effects, the hump in the synthesized glass in Fig. 1 indicates that it is non-crystalline. Ensure that the fabricated samples are amorphous consequently.

Molecular weights and densities are commonly used to evaluate glass density [26–30]. BaO was increased in this study at the expense of LiF. BaO and LiF have molecular masses (153.326 & 25.939), and densities (5.72 &2.64 g/ cm^3). Therefore, density of these samples was increased, as have been reported. The decrease in V_m could be linked to the establishment of (BO), which lessen voids within the structure. ρ & *Vm* of $22SiO_2$- $23Bi_2O_3$-$37B_2O_3$-$13TiO_2$-$(5-x)$ LiF- x BaO glasses are depicted in Fig. 2.

The values of (R_m), ($\propto_m$), (R_L) and (χ), decline with Ba^{+2}, owing to the decrease in V_m, whereas M increases. $\propto°$ and $\wedge$ have the dissimilar value of (χ), so $\propto°$ and $\wedge$ reduces as Ba^{+2} increases. The obtained data values are shown in Table 1.

3.2 Optical Studies

The reflectance (R) has been estimated based on both the optical absorption (A) and transmittance (T). Absorption (A) and transmittance (T) of a glass system are depicted in Fig. 3. The reflectance (R) of fabricated samples is represented in Fig. 4.

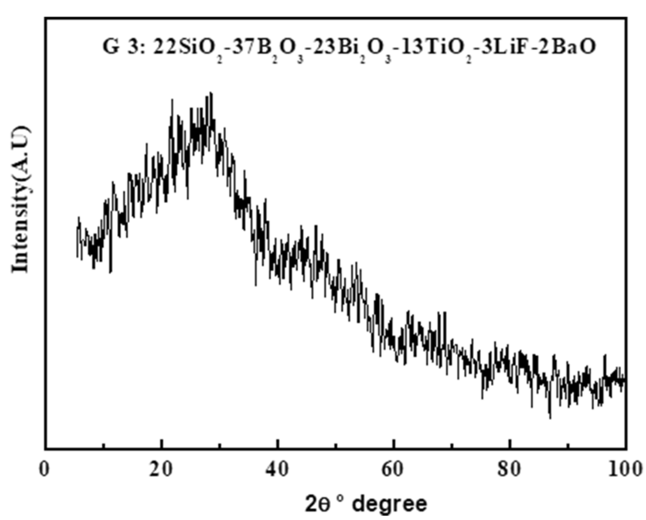

Fig. 1 XRD of $22SiO_2$- $23Bi_2O_3$-$37B_2O_3$-$13TiO_2$-3LiF- 2BaO glasses

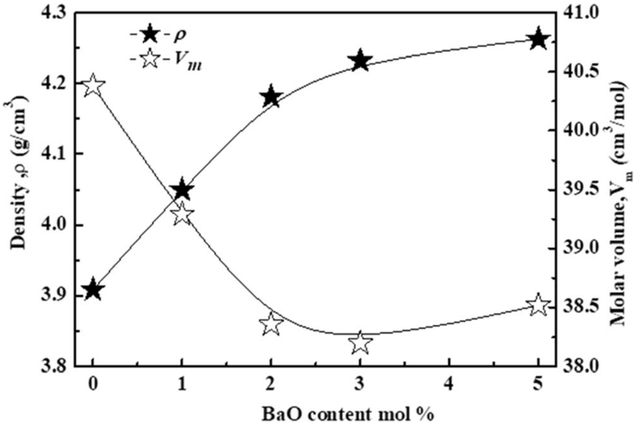

Fig. 2 ρ & Vm of $22SiO_2$- $23Bi_2O_3$-$37B_2O_3$-$13TiO_2$-$(5-x)$ LiF- x BaO glasses

These observations were used to evaluate the absorption coefficient (α), linear &nonlinear bandgap ($E_{opt.}$) Urbach energy (E_U), refractive index (n_D). (α), of these glasses were estimated as: $\propto = (2.303|d) * A$ where d is the sample's thickness. (α), of these glasses was exemplified in Fig. 5. Figure 5 shows an increment as BaO concentration increments, but a decline as light energy increment.

Bandgap energies for direct and indirect transitions, according to Tauc's theory [31–36] are evaluated by:$\alpha h\nu = C(h\nu - E_{opt})^s$. Figs. 6 and 7 present the correlation between ($\alpha h\nu$)$^{1/2}$, ($\alpha h\nu$)^2, and ($h\nu$). The intercepts were used to calculate $E^{dir}_{opt.}$, and $E^{indir}_{opt.}$ for the examined glasses. The obtained data values are shown in Table 1. $E^{dir}_{opt.}$, and $E^{indir}_{opt.}$ both reduced as the BaO content increased. This interpretation may be attributable to the increment in the bond length of Ba-O (1.9397Å) than Li-F (1.57 Å).

E_u of glasses has expected as: $\propto_0 exp\left(\frac{h\nu}{E_u}\right)$. ln(α) versus ($h\nu$), is used to calculate the (E_u) in Fig. 8. The varying relationship stated among their $Eopt$ belongs to E_u. As BaO increases, the E_u increases while the $Eopt$ decreases, as shown in Fig. 8; Table 1.

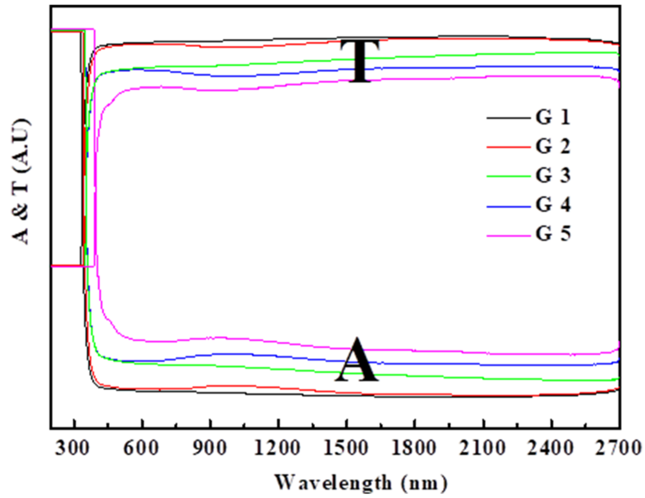

Fig. 3 T & A of $22SiO_2$- $23Bi_2O_3$-$37B_2O_3$-$13TiO_2$-$(5-x)$ LiF- x BaO glasses

Manufacturing glasses have a refractive index as: $n_D = \frac{(1-R)^2+k^2}{(1+R)^2+k^2}$ where $k = \alpha\lambda/4\pi$, and R reflectance and presented in Fig. 9. With increasing BaO content, n_D increases linearly due to increment of density. It stated that ρ and n_D have a meaningful correlation, i.e., the denser the higher n_D value.

Molar Refractivity $R_m = \langle n^2 - 1|n^2 + 2\rangle \; Vm$, molar polarization

$$\propto_m (3|4\pi N)R_m, \text{polarizability} \propto_0^{2-} = \frac{\left[\frac{Vm}{2.52}\left(\frac{n^2-1}{n^2+2}\right) - \sum \propto_{cat}\right]}{N_o^{2-}}$$

, and optical basicity $= 1.67\left(1 - \frac{1}{\propto_0^{2-}}\right)$ were determined. Figures 10 and 11, and 12 illustrate these concepts. These constructs increase as increment BaO concentration,

Table 1 Physical characteristics of $22SiO_2$- $23Bi_2O_3$-$37B_2O_3$-$13TiO_2$-$(5-x)$ LiF- x BaO glasses

Samples	G 1	G 2	G 3	G 4	G 5
N_O	2.5	2.51	2.52	2.53	2.55
R_m (cm^3/mol)	24.3	23.8	23.5	23.61	24.58
$\propto_m$ (A^{o3})	9.65	9.46	9.34	9.366	9.749
(R_L)	0.6	0.61	0.61	0.618	0.638
(M)	0.4	0.39	0.39	0.382	0.362
(χ)	0.85	0.83	0.802	0.784	0.704
(α°)	2.74	2.75	2.78	2.795	2.87
()	1.28	1.285	1.3	1.31	1.35
$E^{indir}_{opt.}$ (e.V)	3.16	3.09	2.985	2.915	2.62
$E^{dir}_{opt.}$, (e.V)	3.52	3.31	3.22	3.19	2.82
E_u (eV)	0.339	0.357	0.367	0.376	0.398

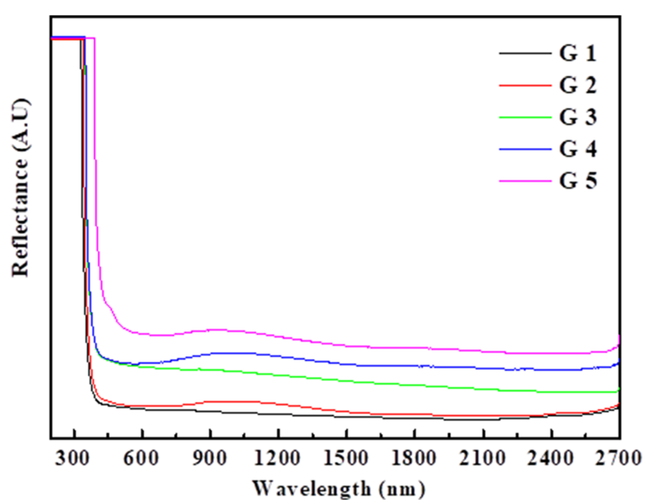

Fig. 4 R of $22SiO_2$- $23Bi_2O_3$-$37B_2O_3$-$13TiO_2$-$(5-x)$ LiF-x BaO glasses

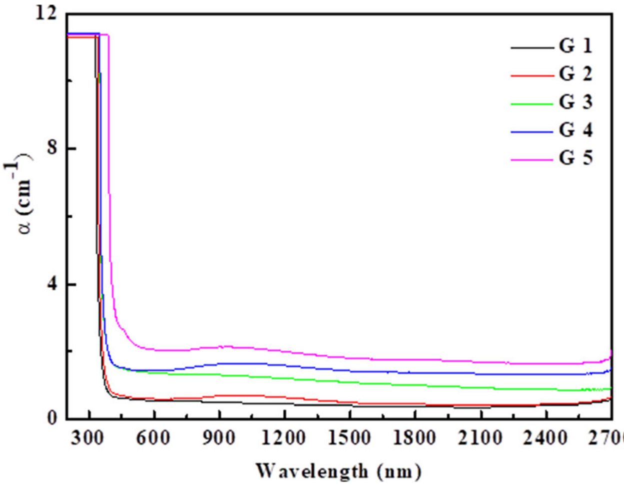

Fig. 5 (α), of $22SiO_2$- $23Bi_2O_3$-$37B_2O_3$-$13TiO_2$-$(5-x)$ LiF- x BaO glasses

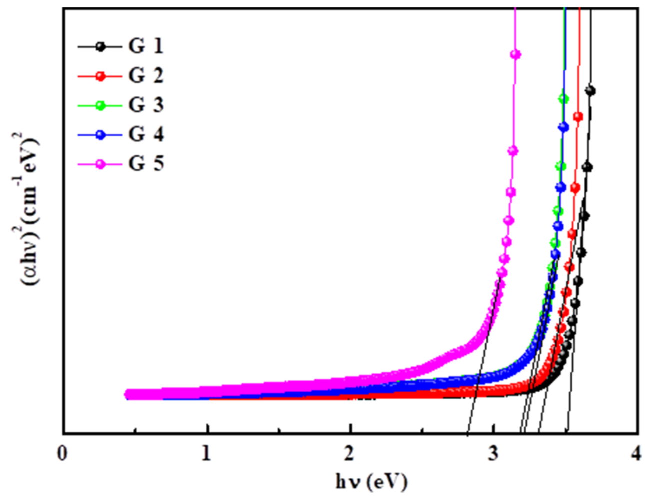

Fig. 7 $(\alpha h\nu)^2$ versus $(h\nu)$, for $22SiO_2$- $23Bi_2O_3$-$37B_2O_3$-$13TiO_2$-$(5-x)$ LiF- x BaO glasses

according to the results of these glasses. The R_m, $\propto_0^{2-}$, and of having the same direction of $Randn_D$. As a result of the increase in BaO, these samples are more polarized. R_m, $\propto_0^{2-}$, and values are increased due to higher polarizability of BaO (3.652) than LiF (3.099) [37–40].

Eo and Ed dispersion was determined by [39–42], $n^2-1=\frac{E_0E_d}{E_0^2-E^2}$,. The slope and intercept of Fig. 13 predict Eo and Ed. $Eopt$, (no), ϵ_∞, (λo), and (So) were calculated as: $Eopt=\frac{E_d}{2}$, $n_0=\sqrt{1+\frac{E_d}{E_0}}$, $\epsilon_\infty=n_0^2andn^2-1=\frac{S_0\lambda_0^2}{1-(\frac{\lambda_0}{\lambda})2}$. Where $Eopt$, energy gap, (no), static refractive index, ϵ_∞, (λo), wavelength, and (So) strength of the oscillator. Table 2 lists these characteristics.

The refractive index (linear and non-linear) is shown in Figs. 14 and 15 [43–48]. $E_{opt.}^{dir}$, and $E_{opt.}^{indir}$ resulting in a minor deviation in the (n_D). Furthermore, the dielectric and the static dielectric constant ($\boldsymbol{o}$, and ∞) were determined as: $\boldsymbol{o}=-33.26876+78.61805E_g-45.70795E_g^2+8.32449E_g^3$, $\infty=n_{AV}^2$. Tables 3 and 4 show the effects of $E_{opt.}^{dir}$, and $E_{opt.}^{indir}$ on various optical constrictions. $(\varepsilon\infty)$, (ε_o), $\chi^{(1)}$, $(\chi^{(3)})$ and (n_2).

3.3 DTA Investigation

We used a differential thermal analyzer to investigate the glass's thermal stability [49–55]. In DTA, the glass transition temperature (T_g), crystallization temperature (T_c), and (T_p) are all crucial. T_g which is defined as the temperature range in which a solid material's behavior changes from solid to liquid. T_c is the temperature at which the viscosity of the glass is low enough to prevent rabid crystal growth. T_p is the temperature at which glass crystal formation occurs. The value of (T_c-T_g) has been used to determine the samples' thermal stability (ΔT), so it is preferable to have a large value for (T_c-T_g) [49–55]. For $22SiO_2$- $23Bi_2O_3$-$37B_2O_3$-$13TiO_2$-$(5-x)$ LiF-

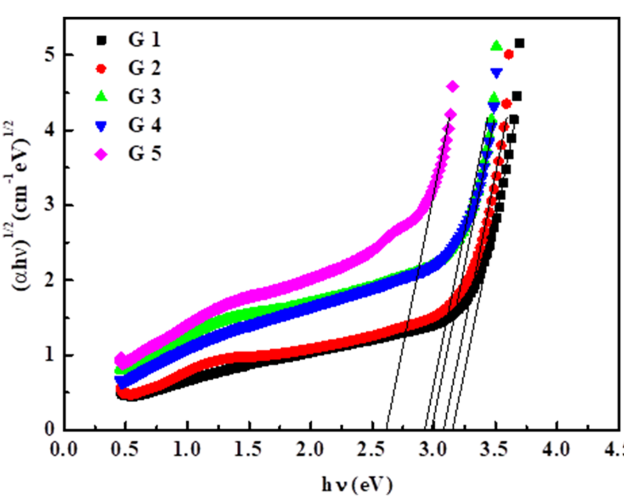

Fig. 6 $(\alpha h\nu)^{1/2}$ versus $(h\nu)$, for $22SiO_2$- $23Bi_2O_3$-$37B_2O_3$-$13TiO_2$-$(5-x)$ LiF- x BaO glasses

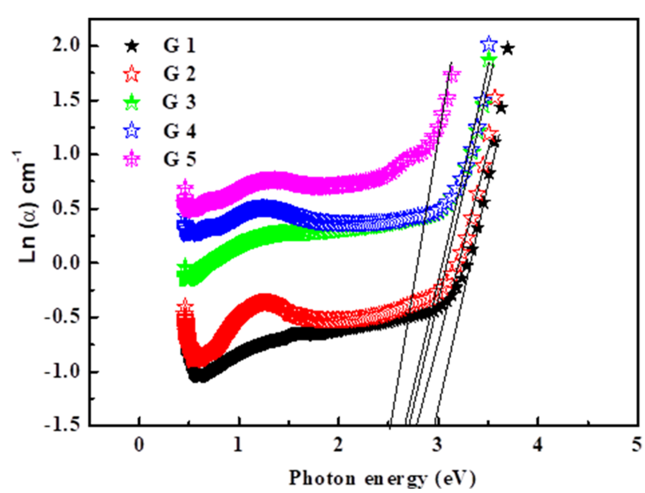

Fig. 8 ln(α) versus $(h\nu)$, for $22SiO_2$- $23Bi_2O_3$-$37B_2O_3$-$13TiO_2$-$(5-x)$ LiF- x BaO glasses

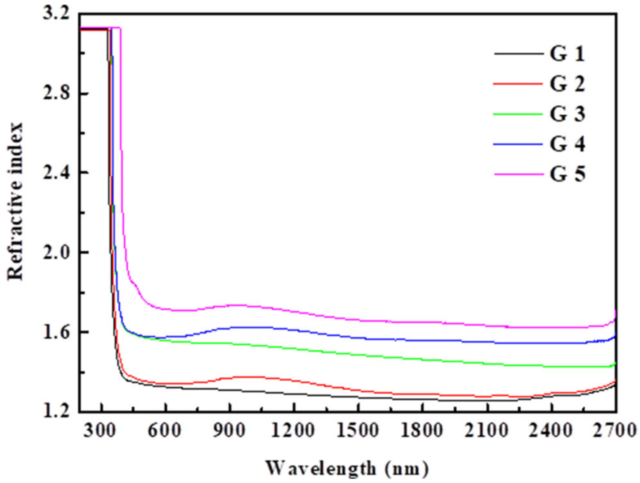

Fig. 9 n_D for $22SiO_2$- $23Bi_2O_3$-$37B_2O_3$-$13TiO_2$-$(5-x)$ LiF- x BaO glasses

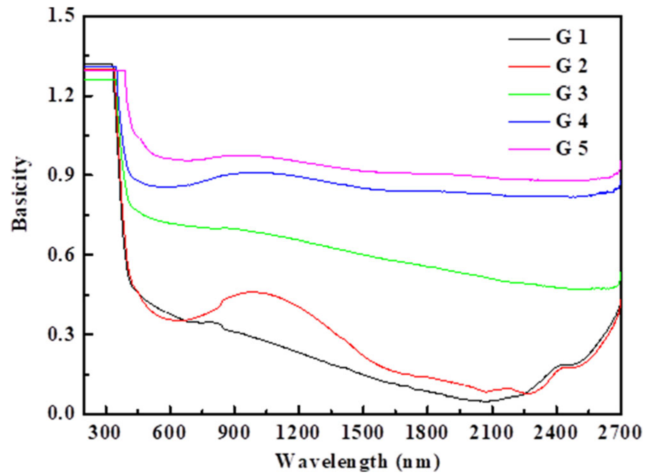

Fig. 12 for $22SiO_2$- $23Bi_2O_3$-$37B_2O_3$-$13TiO_2$-$(5-x)$ LiF- x BaO glasses

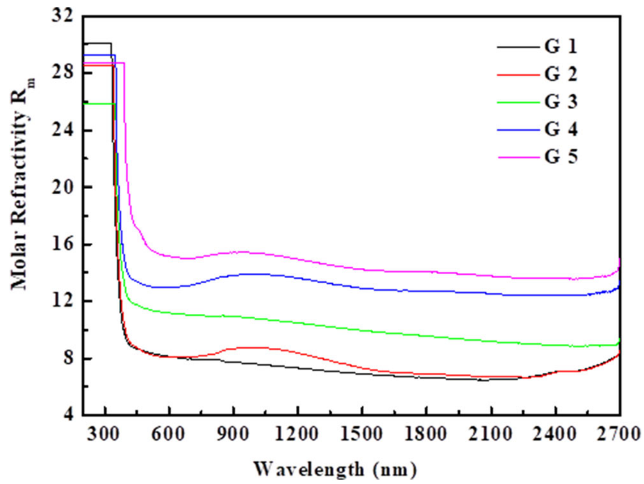

Fig. 10 R_m for $22SiO_2$- $23Bi_2O_3$-$37B_2O_3$-$13TiO_2$-$(5-x)$ LiF- x BaO glasses

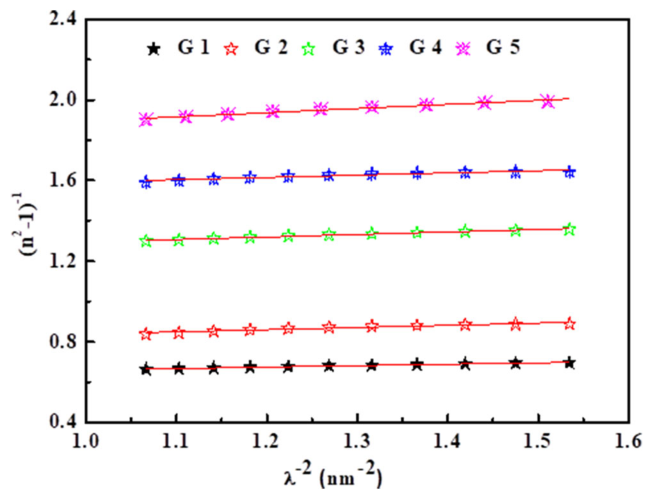

Fig. 13 (n^2-1) versus λ^{-2} for $22SiO_2$- $23Bi_2O_3$-$37B_2O_3$-$13TiO_2$-$(5-x)$ LiF-x BaO glasses

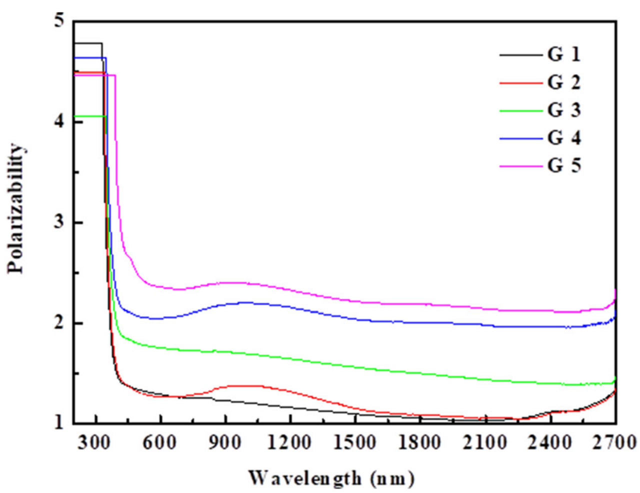

Fig. 11 $\propto_0^{2-}$ for $22SiO_2$- $23Bi_2O_3$-$37B_2O_3$-$13TiO_2$-$(5-x)$ LiF- x BaO glasses

Table 2 E_0, E_d, $Eopt$, no, ϵ_∞, (λo), and (So) values of $22SiO_2$- $23Bi_2O_3$-$37B_2O_3$-$13TiO_2$-$(5-x)$ LiF- x BaO

Sample	E_0	E_d	$Eopt$ (eV)	n_0	ϵ_∞	So (m^{-2})	λo (nm)
G 1	2.47	3.67	1.83	1.576	2.48	1.956	413.97
G 2	2.6	3.06	1.53	1.473	2.17	2.06	477.33
G 3	4.92	2.90	1.45	1.261	1.59	2.03	504
G 4	1.70	2.87	1.44	1.640	2.7	1.986	534.5
G 5	3.54	2.58	1.29	1.315	1.73	2	569.7

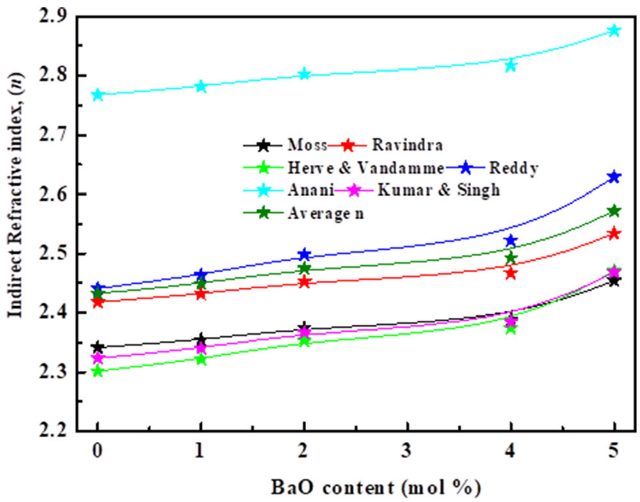

Fig. 14 Non − linearn_D for $22SiO_2$- $23Bi_2O_3$-$37B_2O_3$-$13TiO_2$-(5 − x) LiF- x BaO glasses

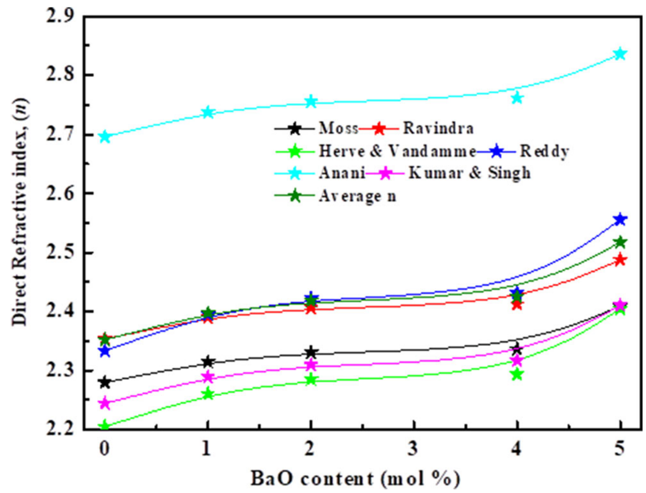

Fig. 15 Linearn_D for $22SiO_2$- $23Bi_2O_3$-$37B_2O_3$-$13TiO_2$-(5 − x) LiF- x BaO glasses

x BaO glasses, typical DTA traces are shown in Fig. 16. Table 5 lists DTA values of $22SiO_2$- $23Bi_2O_3$-$37B_2O_3$-$13TiO_2$-(5 − x) LiF- x BaO glasses.

The resistance to a permanent change in characteristics directly impacted by heat is defined as $\Delta T = (T_c - T_g)$. The resistance of glass to crystallization during heating is referred to as glass stability. The creation of bridging oxygens (BO) increases ΔT (from 123 to 137 °C) as BaO increases, as presented in Table 5. Thermally stable glasses have a ΔT > 100 °C. This indicates that the $22SiO_2$- $23Bi_2O_3$-$37B_2O_3$-$13TiO_2$-(5 − x) LiF- x BaO glasses can be heated above T_g without crystallizing. Thermodynamic stability is also measured by other criteria [56], weighted thermal stability $H_g = \frac{T}{T_g}$. As presented in Table 5 H_g increased (from 0.34 to 0.35 °C), these behaviors indicated that the $22SiO_2$- $23Bi_2O_3$-$37B_2O_3$-$13TiO_2$-(5 − x) LiF- x BaO glasses Thermally stable.

T_g increased (from 360 to 390 °C), T_c increased (from 483 to 527 °C), and T_p increased (from 593 to 618 °C) in the

Table 3 ($\varepsilon\infty$), (ε_o), $\chi^{(1)}$, $(\chi^{(3)})$ and (n_2) value as a function of $E_{opt.}^{indir}$

Sample name	dielectric constant		Nonlinear parameters			F	β absorption coefficient
	ε∞	ε0	$\chi^{(1)}$ (esu)	$(\chi^{(3)})$ 10^{-12} (esu)	(n_2) 10^{-11} (esu)	*F*	β
G 1	5.92	21.42	0.39	3.99	6.18	0.03125	2.378
G 2	5.998	18.84	0.398	4.26	6.5	0.03125	2.509
G 3	6.12	15.54	0.408	4.71	7.17	0.03125	2.73
G 4	6.2	13.7	0.415	5.04	7.62	0.03125	2.88
G 5	6.61	8.67	0.447	6.79	9.94	0.03125	3.7

Table 4 ($\varepsilon\infty$), (ε_o), $\chi^{(1)}$, $(\chi^{(3)})$ and (n_2) value as a function of $E_{opt.}^{dir}$

Sample name	dielectric constant		Nonlinear parameters			F	β absorption coefficient
	ε∞	ε0	F	β	(n_2) 10^{-11} (esu)	*F*	β
G 1	5.53	40.19	0.36	2.88	4.61	0.03125	1.84
G 2	5.75	28.06	0.378	3.48	5.46	0.03125	2.13
G 3	5.85	23.88	0.386	3.77	5.88	0.03125	2.274
G 4	5.88	22.62	0.389	3.88	6.03	0.03125	2.325
G 5	6.34	11.63	0.425	5.54	8.29	0.03125	3.124

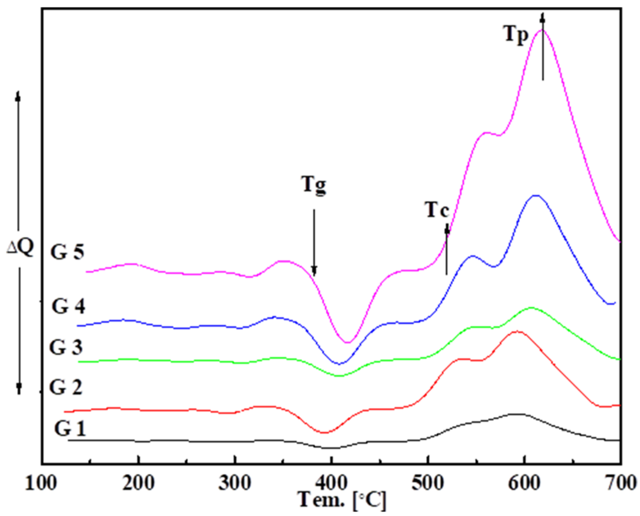

Fig. 16 DTAof 22SiO$_2$- 23Bi$_2$O$_3$-37B$_2$O$_3$-13TiO$_2$-(5 − x) LiF- x BaO glasses

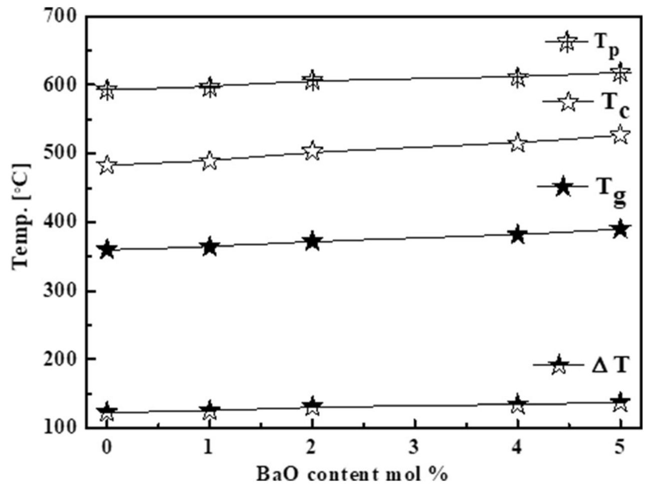

Fig. 17 Parameters of values 2SiO$_2$- 23Bi$_2$O$_3$-37B$_2$O$_3$-13TiO$_2$-(5 − x) LiF- x BaO

current study. It is well known that changes in glass structure affect in (T_g), and ΔT of glasses is visible in close-packed structures. In the current study, LiF was substituted for BaO because single-bond Ba O energy in the glass network is higher than Li F energy, making these glasses more stable. Moreover, BaO has a higher average cross-link density than LiF, which contributes to its superiority. Figure 17 presented DTA of values of 22SiO$_2$- 23Bi$_2$O$_3$-37B$_2$O$_3$-13TiO$_2$-(5 − x) LiF- x BaO glasses with BaO content.

Table 5 DTA of values of 22SiO$_2$- 23Bi$_2$O$_3$-37B$_2$O$_3$-13TiO$_2$-(5 − x) LiF- x BaO glasses (°C)

Sample name	T_g	T_c	T_p	ΔT	H_g
G 1	360	483	593	123	0.34
G 2	364	489	597	125	0.34
G 3	372	503	607	131	0.35
G 4	381	515	611	134	0.35
G 5	390	527	618	137	0.35

4 Conclusions

Using melt-quenching techniques, the glass system 22SiO$_2$- 23Bi$_2$O$_3$-37B$_2$O$_3$-13TiO$_2$ − (5 − x) LiF- x BaO was prepared. The influences of BaO on the thermal and optical characteristics of fabricated glasses were investigated in the current article. The fabricated samples are amorphous, according to XRD analysis. In this manuscript, the molar volume is reduced while the density is raised. The thermal stability of fabricated glasses is mainly affected by changes in glass network connectivity. In the current study, LiF was substituted for BaO because single-bond Ba O energy in the glass network is higher than Li F energy, making these glasses more stable. Moreover, BaO has a higher average cross-link density than LiF, which contributes to its superiority. Therefore, as BaO levels rise, all the thermal parameters rise as well. The fabricated glass samples showed a decrease in optical bandgap $E^{dir}_{opt.}$, and $E^{indir}_{opt.}$ while (E_u) increased. Molar refractivity, molar polarization, polarizability, and optical basicity all decrease as BaO content rises. Using the Wemple and Didomenico principles, the $E_{0,}$ E_d, $Eopt, no$, ϵ_∞, (λo), and (So) dispersion parameters were determined.

Acknowledgements We would like to thank Taif University Research Supporting Project number (TURSP-2020/24), Taif University, Taif, Saudi Arabia. Moreover, the authors express their gratitude to the Deanship of Scientific Research at King Khalid University for funding this work through research groups program under grant number R.G.P. 2/137/42.

Author Contributions Kh. S. Shaaban: Conceptualization, Methodology, Writing Reviewing Discussion and Editing helping in reviewers' responses. Z.A. Alrowaili, Ateyyah M. Al-Baradi, Atif Mossad Ali, E. A. Abdel Wahab, M.S. Al-Buriahi, Editing helping in reviewers' responses.

Data Availability My manuscript and associated personal data.

Declarations The manuscript has not been published.

Conflict of Interest The authors declare that they have no conflict of interest.

Declaration of Competing Interest The authors declare that they have no known competing financial interests.

Consent to Participate The authors consent to participate.

Consent for Publication The author's consent for publication.

References

1. Pu Z, Huang J, Li J, Feng H, Wang X, Yin X (2021) Effect of F content on the structure, viscosity and dielectric properties of SiO_2-Al_2O_3-B_2O_3-RO-TiO_2 glasses. J Non-Cryst Solids 563:120817. https://doi.org/10.1016/j.jnoncrysol.2021.120817
2. Ruengsri S, Kaewkhao J, Limsuwan P (2012) Optical Characterization of Soda Lime Borosilicate Glass Doped with TiO_2, Procedia Eng 32(2012):772–779. https://doi.org/10.1016/j.proeng.2012.02.011
3. Mahmoud KH, Alsubaie AS, Wahab EAA, Abdel-Rahim FM, Shaaban KS (2021) Research on the effects of yttrium on bismuth Titanate Borosilicate glass system. Silicon. https://doi.org/10.1007/s12633-021-01125-0
4. Shaaban KS, Al-Baradi AM, Wahab EAA (2021) The impact of Y_2O_3 on physical and optical characteristics, polarizability, optical basicity, and dispersion parameters of $B_2O_3 – SiO_2 – Bi_2O_3 – TiO_2$ glasses. Silicon. https://doi.org/10.1007/s12633-021-01309-8
5. Al-Baradi AM, Wahab EAA, Shaaban KS (2021) Preparation and characteristics of $B_2O_3 – SiO_2 – Bi_2O_3 – TiO_2 – Y_2O_3$ glasses and glass-ceramics. Silicon. https://doi.org/10.1007/s12633-021-01286-y
6. Shaaban KS, Abo-Naf SM, Hassouna MEM (2019) Physical and structural properties of lithium borate glasses containing MoO_3. Silicon 11:2421–2428. https://doi.org/10.1007/s12633-016-9519-4
7. Sayed MA, Ali AM, Abd El-Rehim AF, Abdel Wahab EA, Shaaban KS (2021) Dispersion parameters, polarizability, and basicity of lithium phosphate glasses. J Electron Mater. https://doi.org/10.1007/s11664-021-08921-9
8. Wahab EAA, Aboraia AM, Shafey AME, Shaaban KS, Soldatov AV (2021) The effect of ZrO_2 on the linear and non-linear optical properties of sodium silicate glass. Opt Quant Electron 53. https://doi.org/10.1007/s11082-021-03164-8
9. El-Rehim AFA, Wahab EAA, Halaka MMA, Shaaban KS (2021) Optical Properties of $SiO_2 – TiO_2 – La_2O_3 – Na_2O – Y_2O_3$ Glasses and A Novel Process of Preparing the Parent Glass-Ceramics. Silicon. https://doi.org/10.1007/s12633-021-01002-w
10. Scannell G, Barra S, Huang L (2016) Structure and properties of Na_2O-TiO_2-SiO_2 glasses: Role of Na and Ti on modifying the silica network. J Non-Cryst Solids 448:52–61. https://doi.org/10.1016/j.jnoncrysol.2016.06.028
11. Somaily HH, Shaaban KS, Makhlouf SA, Algarni H, Hegazy HH, Wahab EAA, Shaaban ER (2021) Comparative studies on polarizability, optical basicity and optical properties of lead borosilicate modified with titania. J Inorg Organomet Polym Mater 31:138–150. https://doi.org/10.1007/s10904-020-01650-2
12. Shaaban KS, Wahab EAA, Shaaban ER, Yousef ES, Mahmoud SA (2020) Electronic polarizability, optical basicity, thermal, mechanical and optical investigations of $(65B_2O_3–30Li_2O–5Al_2O_3)$ glasses doped with titanate. J Electron Mater 49:2040–2049. https://doi.org/10.1007/s11664-019-07889-x
13. Shaaban KS, Yousef ES, Mahmoud SA, Wahab EAA, Shaaban ER (2020) Mechanical, structural and crystallization properties in titanate doped phosphate glasses. J Inorg Organomet Polym Mater 30:4655–4663. https://doi.org/10.1007/s10904-020-01574-x
14. Shaaban KS, Koubisy MSI, Zahran HY, Yahia IS (2020) Spectroscopic properties, electronic polarizability, and optical basicity of titanium–cadmium tellurite glasses doped with different amounts of lanthanum. J Inorg Organomet Polym Mater 30:4999–5008. https://doi.org/10.1007/s10904-020-01640-4
15. El-Rehim AFA, Zahran HY, Yahia IS, Wahab EAA, Shaaban KS (2021) Structural, elastic moduli, and radiation shielding of SiO_2-TiO_2-La_2O_3-Na_2O glasses containing Y_2O_3. J Mater Eng Perform 30:1872–1884. https://doi.org/10.1007/s11665-021-05513-w
16. Strimple JH, Giess EA, (1958), Glass formation and properties of glasses in the system Na_2O-B_2O_3-SiO_2-TiO_2. J Am Ceram Soc 41(7):231-237. https://doi.org/10.1111/j.1151-2916.1958.tb13546.x
17. Limbach R, Karlsson S, Scannell G, Mathew R, Edén M, Wondraczek L (2017) The effect of TiO_2 on the structure of Na_2O-CaO-SiO_2 glasses and its implications for thermal and mechanical properties. J Non-Cryst Solids 471:6–18. https://doi.org/10.1016/j.jnoncrysol.2017.04.013
18. Shaaban KS, Saddeek YB, Sayed MA, Yahia IS, (2018). Mechanical and thermal properties of lead borate glasses containing CaO and NaF. Silicon 10:1973–1978. https://doi.org/10.1007/s12633-017-9709-8
19. Yamane M, Kawazoe H, Inoue S, Maeda K (1985) IR transparency of the glass of $ZnCl_2$-KBr-$PbBr_2$ system. Mater Res Bull 20:905–911. https://doi.org/10.1016/0025-5408(85)90073-x
20. Abdelghany AM, Elbatal HA, Ezzeldin FM (2015) Influence of CuO content on the structure of lithium fluoroborate glasses: Spectral and gamma irradiation studies. Spectrochim Acta Part A Mol Biomol Spectrosc 149:788–792. https://doi.org/10.1016/j.saa.2015.04.105
21. Rammah YS, El-Agawany FI, Elkhoshkhany N, Elmasry F, Reben M, Grelowska I, Yousef E (2021) Physical, optical, thermal, and gamma-ray shielding features of fluorotellurite lithiumniobate glasses: TeO_2-$LiNbO_3$-BaO-BaF_2-La_2O_3 J Mater Sci: Mater Electron 32:3743–3752. https://doi.org/10.1007/s10854-020-05119-3
22. Elbatal FHA, Marzouk MA, Hamdy YM, Elbatal HA (2014) Optical and FT infrared absorption spectra of 3d transition metal ions doped in NaF-CaF_2-B_2O_3 glass and effects of gamma irradiation. J Solid-State Phys 2014:1–8. https://doi.org/10.1155/2014/389543
23. El-Rehim AFA, Shaaban KS (2021) Influence of La_2O_3 content on the structural, mechanical, and radiation-shielding properties of sodium fluoro lead barium borate glasses. J Mater Sci: Mater Electron 32:4651–4671. https://doi.org/10.1007/s10854-020-05204-7
24. Shaaban KS, Alomairy S, Al-Buriahi MS (2021) Optical, thermal and radiation shielding properties of B_2O_3–NaF–PbO–BaO–La_2O_3 glasses. J Mater Sci: Mater Electron. https://doi.org/10.1007/s10854-021-05885-8
25. Shaaban KS, Saddeek YB (2017) Effect of MoO_3 content on structural, thermal, mechanical and optical properties of (B_2O_3-SiO_2-Bi_2O_3-Na_2O-Fe_2O_3) glass system. Silicon 9:785–793. https://doi.org/10.1007/s12633-017-9558-5
26. Shaaban KS, Abdel Wahab EA, El-Maaref AA, Abdelawwad M, Shaaban ER, Yousef ES, Wilke H, Hillmer H, Börcsök J (2020) Judd–Ofelt analysis and physical properties of erbium modified cadmium lithium gadolinium silicate glasses. J Mater Sci: Mater Electron 31:4986–4996. https://doi.org/10.1007/s10854-020-03065-8
27. Shaaban KS, Zahran HY, Yahia IS, Elsaeedy HI, Shaaban ER, Makhlouf SA, Wahab EAA, Yousef ES (2020) Mechanical and radiation-shielding properties of B_2O_3–P_2O_5–Li_2O–MoO_3 glasses. Appl Phys A 126. https://doi.org/10.1007/s00339-020-03982-9
28. Saudi HA, Abd-Allah WM, Shaaban KS (2020) Investigation of gamma and neutron shielding parameters for borosilicate glasses doped europium oxide for the immobilization of radioactive waste. J Mater Sci: Mater Electron 31:6963–6976. https://doi.org/10.1007/s10854-020-03261-6
29. Fayad AM, Shaaban KS, Abd-Allah WM, Ouis M (2020) Structural and optical study of CoO doping in borophosphate host glass and effect of gamma irradiation. J Inorg Organomet Polym Mater 30:5042–5052. https://doi.org/10.1007/s10904-020-01641-3
30. Abd-Allah WM, Saudi HA, Shaaban KS, Farroh HA (2019) Investigation of structural and radiation shielding properties of

$40B_2O_3$–30PbO–(30-x) BaO-x ZnO glass system. Appl Phys A 125. https://doi.org/10.1007/s00339-019-2574-0

31. Nayak MT, Desa JAE, Reddy VR, Nayak C, Bhattacharyya D, Jha SN (2019) Structural studies of potassium silicate glasses with fixed iron content and their relation to similar alkali silicates. J Non-Cryst Solids 518:85–91. https://doi.org/10.1016/j.jnoncrysol.2019.04.025
32. Wahab EAA, Shaaban KS (2018) Effects of SnO_2 on spectroscopic properties of borosilicate glasses before and after plasma treatment and its mechanical properties. Mater Res Express 5(2):025207. https://doi.org/10.1088/2053-1591/aaaee8
33. Abdel Wahab EA, Koubisy MSI, Sayyed MI, Mahmoud KA, Zatsepin AF, Makhlouf SA, Shaaban KhS (2021) Novel borosilicate glass system: $Na_2B_4O_7$-SiO_2-MnO_2 Synthesis, average electronics polarizability, optical basicity, and gamma-ray shielding features, J Non-Cryst Solids 553:120509. https://doi.org/10.1016/j.jnoncrysol.2020.120509
34. El-Rehim AFA, Wahab EAA, Halaka MMA, Shaaban KS (2021) Optical properties of $SiO_2 – TiO_2 – La_2O_3 – Na_2O – Y_2O_3$ glasses and a novel process of preparing the parent glass-ceramics. Silicon. https://doi.org/10.1007/s12633-021-01002-w
35. Shaaban KS, Boukhris I, Kebaili I, Al-Buriahi MS (2021) Spectroscopic and attenuation shielding studies on B_2O_3-SiO_2-LiF-ZnO-TiO_2 glasses. Silicon. https://doi.org/10.1007/s12633-021-01080-w
36. Abdel Wahab EA, Shaaban KS, Yousef ES (2020) Enhancement of optical and mechanical properties of sodium silicate glasses using zirconia. Opt Quant Electron 52. https://doi.org/10.1007/s11082-020-02575-3
37. Shaaban KS, Wahab EAA, Shaaban ER, Yousef ES, Mahmoud SA (2020) Electronic polarizability, optical basicity and mechanical properties of aluminum lead phosphate glasses. Opt Quant Electron 52. https://doi.org/10.1007/s11082-020-2191-3
38. Azlan MN, Halimah MK, Suriani AB, Azlina Y, El-Mallawany R (2019) Electronic polarizability and third-order nonlinearity of Nd^{3+} doped borotellurite glass for potential optical fiber. Mater Chem Phys 236:121812. https://doi.org/10.1016/j.matchemphys.2019.121812
39. Wemple SH, DiDomenico M Jr (1971) Behavior of the electronic dielectric constant in covalent and ionic materials. Phys Rev B 3:1338–1351. https://doi.org/10.1103/PhysRevB.3.1338
40. Abdel-Aziz MM, Yahia IS, Wahab LA, Fadel M, Afifi MA (2006) Determination and analysis of dispersive optical constant of TiO_2 and Ti_2O_3 thin films. Appl Sur Sci 252(23):8163–8170. https://doi.org/10.1016/j.apsusc.2005.10.040
41. Abdel-Aziz MM, Metwally EG, El-, Fadel M, Labib HH, Afifi MA (2001) Optical properties of amorphous Ge-Se-Tl system films. Thin Solid Films 386:99–104. https://doi.org/10.1016/S0040-6090(01)00765-9
42. Chiad SS, Habubi NF, Abass WH, Abdul Allah MH (2016) Effect of thickness on the optical and dispersion parameters of $Cd_{0.4}Se_{0.6}$ thin films. J Opt Elec Adv Mat 18(9–10):822
43. Moss TS (1985) Relations between the refractive index and energy gap of semiconductors. Phys Status Solidi (b) 131(2):415–427. https://doi.org/10.1002/pssb.2221310202
44. Ravindra NM (1981) Energy gap-refractive index relation — some observations. Infrared Phys 21(5):283–285. https://doi.org/10.1016/0020-0891(81)90033-6
45. Gupta VP, Ravindra NM (1980) Comments on the moss formula. Phys Status Solidi (b) 100(2):715–719. https://doi.org/10.1002/pssb.2221000240
46. Anani M, Mathieu C, Lebid S, Amar Y, Chama Z, Abid H (2008) Model for calculating the refractive index of a III-V semiconductor. Comput Mater Sci 41:570–757
47. Kumar V, Singh JK (2010) Model for calculating the refractive index of different materials. Ind J Pure Appl Phys 48:571–574
48. Hervé P, Vandamme LKJ (1994) General relation between refractive index and energy gap in semiconductors. Infrared Phys Technol 35(4):609–615. https://doi.org/10.1016/1350-4495(94)90026-4
49. El-Rehim AFA, Ali AM, Zahran HY, Yahia IS, Shaaban KS (2021) Spectroscopic, structural, thermal, and mechanical properties of B_2O_3-CeO_2-PbO_2 glasses. J Inorg Organomet Polym Mater 31:1774–1786. https://doi.org/10.1007/s10904-020-01799-w
50. Shaaban KS, Yousef ES, Abdel Wahab EA, Shaaban ER, Mahmoud SA (2020) Investigation of crystallization and mechanical characteristics of glass and glass-ceramic with the compositions xFe_2O_3-$35SiO_2$-$35B_2O_3$-$10Al_2O_3$-(20–x) Na_2O. J Mater Eng Perform 29:4549–4558. https://doi.org/10.1007/s11665-020-04969-6
51. Shaaban KS, Abo-Naf SM, Abd Elnaeim AM, Hassouna MEM (2017) Studying effect of MoO_3 on elastic and crystallization behavior of lithium diborate glasses. Appl Phys A 123. https://doi.org/10.1007/s00339-017-1052-9
52. Shaaban KS, Yousef ES (2020) Optical properties of Bi_2O_3 doped boro tellurite glasses and glass ceramics. Optik 203:163976. https://doi.org/10.1016/j.ijleo.2019.163976
53. El-Rehim AFA, Zahran HY, Yahia IS, Makhlouf SA, Shaaban KS (2021) Radiation, crystallization, and physical properties of cadmium borate glasses. Silicon 13:2289–2307. https://doi.org/10.1007/s12633-020-00798-3
54. El-Rehim AFA, Zahran HY, Yahia IS, Ali AM, Shaaban KS (2020) Physical, radiation shielding and crystallization properties of Na_2O-Bi_2O_3- MoO_3-B_2O_3- SiO2-Fe_2O_3 glasses. Silicon. https://doi.org/10.1007/s12633-020-00827-1
55. Novatski A, Somer A, Gonçalves A, Piazzetta RLS, Gunha JV, Andrade AVC, Lenzi EK, Medina AN, Astrath NGC, El-Mallawany R (2019) Thermal and optical properties of lithium-zinc-tellurite glasses. Mater Chem Phys 231:150–158. https://doi.org/10.1016/j.matchemphys.2019.03.078
56. Saad M, Poulain M (1987) Glass forming ability criterion. Mater Sci Forum:19–20:11–18. https://doi.org/10.4028/www.scientific.net/msf.19-20.11